Title:

Netrin signaling mediates survival of dormant epithelial ovarian cancer cells

Authors:

Pirunthan Perampalam[1,2], James I. MacDonald[1,3], Komila Zakirova[1,3], Daniel T. Passos[1,3], Yudith Ramos-Valdes[1,4], Maëva Hervieu[5], Patrick Mehlen[5,6], Rob Rottapel[7,8], Benjamin Gibert[5], Rohann Correa[1,9], Trevor G. Shepherd[1,4,9,10,11], Frederick A. Dick[1,3,9,12,13]

Affiliations:

1. London Regional Cancer Program, London Health Sciences Centre Research Institute, London, Ontario, Canada, N6A 4L6.
2. Department of Biochemistry, University of Western Ontario, London, ON, Canada, N6A 5C1.
3. Department of Pathology and Laboratory Medicine, University of Western Ontario, London, ON, Canada, N6A 5C1.
4. The Mary and John Knight Translational Ovarian Cancer Research Unit, London Regional Cancer Program, London, Ontario, Canada, N6A 4L6.
5. Apoptosis, Cancer and Development Laboratory - Equipe labellisée 'La Ligue', LabEx DEVweCAN, Institut Convergence PLAsCAN, Centre de Recherche en Cancérologie de Lyon (CRCL), INSERM U1052-CNRS UMR5286, Université de Lyon, Université Claude Bernard Lyon1, Centre Léon Bérard, 69008 Lyon, France.
6. Netris Pharma, 69008 Lyon, France
7. Princess Margaret Cancer Centre, University Health Network, 101 College Street, Toronto, Ontario, Canada, M5G 1L7
8. Department of Medical Biophysics, University of Toronto, 1 King's College Circle, Toronto, Ontario, Canada, M5S 1A8
9. Department of Oncology, Western University, London, Ontario, Canada, N6A 4L6.
10. Department of Obstetrics and Gynecology, Western University, London, Ontario, Canada, N6A 5W9.
11. Department of Anatomy and Cell Biology, Western University, London, Ontario, Canada, N6A 5C1.
12. Children's Health Research Institute, London, Ontario, Canada, N6A 4V2.
13. Correspondence: fdick@uwo.ca

Keywords:
Netrin, high grade serous ovarian cancer, DYRK1A, dormancy, quiescence, spheroids

Conflict of interest statement:
P. Mehlen is the founder and CEO of Netris Pharma and has an ownership interest including stocks and patents. The other authors have declared that no conflict of interest exists.

Abstract

Dormancy in cancer is a clinical state in which residual disease remains undetectable for a prolonged duration. At a cellular level, rare cancer cells cease proliferation and survive chemotherapy and disseminate disease. We utilized a suspension culture model of high grade serous ovarian cancer (HGSOC) cell dormancy and devised a novel CRISPR screening approach to identify genetic requirements for cell survival under growth arrested and spheroid culture conditions. In addition, multiple RNA-seq comparisons were used to identify genes whose expression correlates with survival in dormancy. Combined, these approaches discover the Netrin signaling pathway as critical to dormant HGSOC cell survival. We demonstrate that Netrin-1 and -3, UNC5H receptors, DCC and other fibronectin receptors induce low level ERK activation to promote survival in dormant conditions. Furthermore, we determine that Netrin-1 and -3 overexpression is associated with poor prognosis in HGSOC and demonstrate their overexpression elevates cell survival in dormant conditions. Lastly, Netrin-1 or -3 overexpression contributes to greater spread of disease in a xenograft model of abdominal dissemination. This study highlights Netrin signaling as a key mediator HGSOC cancer cell dormancy and metastasis.

57 **Introduction**

58 Relapse from initially effective cancer treatment represents one of the greatest barriers to
59 improving outcomes (1). Dormant or minimal residual disease that is not clinically detectable is
60 a common source of relapse, particularly in a metastatic setting (2). This has motivated the
61 search for, and study of, disseminated cancer cells. Cellular dormancy has been characterized in
62 cancer cells derived from a variety of primary disease sites including breast, prostate, melanoma,
63 and others (3, 4). Disseminated cells often occupy specific cellular niches in perivascular space
64 or in bone marrow (5), they adopt catabolic metabolism (2), and withdraw from the cell cycle
65 (4). Stem like phenotypes and epithelial to mesenchymal transition also characterize the biology
66 of these cells as they survive dissemination and lay quiescent in distant tissues (1, 3, 5). Across a
67 variety of disease sites this dormant state is characterized by diminished Ras-MAPK signaling
68 and elevated p38 activity (3, 6). To develop treatments specifically tailored for dormant cells, a
69 systematic search for vulnerabilities unique to dormancy is needed. To this end, high grade
70 serous ovarian cancer disseminates as growth arrested cellular aggregates that are amenable to
71 modeling in culture (7), suggesting they are ideal to search for survival dependencies of dormant
72 cells.

73 High grade serous ovarian cancer (HGSOC) is the deadliest gynecologic malignancy,
74 accounting for more than 70% of cases (8). Its poor prognosis is largely attributed to late-stage
75 diagnosis with metastases already present. Metastatic spread is facilitated by multicellular
76 clusters of tumor cells, called spheroids, that are shed into the peritoneal cavity and disseminate
77 to nearby organs (9). The non-proliferative state of spheroid cells renders them chemoresistant
78 and contributes to disease recurrence, emphasizing the need to understand the biology of these
79 cells (10). Dormant HGSOC cells are characterized by similar metabolic changes, EMT, and

80 cytokine signaling as dormant cancer cells from other disease sites (3, 11). Mechanisms that
81 mediate their dormant properties include AMPK-LKB1 signaling that induces autophagy (12,
82 13), STAT3 and FAK for survival and chemoresistance (14, 15), and DYRK1A signaling to
83 arrest proliferation (16). Unfortunately, therapeutic approaches to target these pathways in
84 ovarian cancer have yet to emerge, indicating that more candidates are needed.

85 Netrins are a family of secreted factors that reside in the extracellular matrix around cells
86 and were first identified in axon guidance in the developing nervous system (17, 18). Together
87 with their receptors, Netrins have since been implicated in cancer progression (19). Netrin-1 is
88 the most studied and its misregulation in cancer leads to pro-survival signals (20). Netrin
89 interactions with DCC and UNC5 homologs (UNC5H, UNC5A-D) convert pro-death signals by
90 these dependence receptors to survival signals (21). Netrin signals through PI3K-AKT and
91 ERK-MAPK are known to participate in growth and orientation by providing guidance cues (22-
92 24), while loss of ligand binding leads DCC or UNC5H to stimulate dephosphorylation of
93 DAPK1 that sends pro-death signals (25, 26). The gene encoding DCC is frequently deleted in
94 cancer (20), and Netrin-1 blocking antibodies are in Phase II clinical trials for endometrial and
95 cervical carcinomas to inhibit metastatic growth (21). Alternative receptors for Netrins such as
96 NEO, DSCAM, and Integrins also mediate their signals (19), creating a myriad of possible
97 signaling pathways for Netrins to regulate cancer cells. Lastly, functional roles for Netrin-3, -4,
98 and -5 are still relatively unexplored compared to Netrin-1 (27), although their expression
99 patterns suggest roles in advanced forms of some cancers (28). A functional role for Netrins and
100 their receptors in dormancy, or other aspects of HGSOC spheroid biology have yet to be
101 reported.

102 In this study we utilized a suspension culture system to interrogate survival mechanisms
103 in dormancy using HGSOC spheroids. To maximize discovery of gene loss events that
104 compromise viability in dormancy, we devised a novel genome-wide CRISPR screen approach
105 that we term 'GO-CRISPR'. In addition to the standard CRISPR workflow, GO-CRISPR
106 utilizes a parallel screen in which 'guide-only' cells lacking Cas9 are used to control for
107 stochastic changes in gRNA abundance in non-proliferative cells. This screen identified multiple
108 Netrin ligands, DCC, UNC5Hs, and downstream MAPK signaling components as supporting
109 survival of HGSOC cells in dormant culture conditions. A transcriptomic analysis of HGSOC
110 spheroids also revealed Netrin signaling components were enriched in HGSOC spheroids
111 compared to adherent cells, and that in the absence of the DYRK1A survival kinase Netrin
112 transcriptional increases were lost. We show that multiple Netrins, UNC5 receptors, and the
113 downstream MEK-ERK axis is crucial for survival signaling in dormancy. Overexpression of
114 Netrin-1 and -3 are associated with poor prognosis in HGSOC and their overexpression in
115 culture increases survival in dormant suspension culture. Lastly, we demonstrate that Netrin
116 signaling contributes to disease dissemination in a xenograft model of metastasis. Our study
117 highlights Netrin-ERK signaling as a requirement for spheroid survival and suggests it may be a
118 potential therapeutic target for eradicating dormant HGSOC cells.

119 **Results**

120 ***Axon guidance genes are essential factors for EOC spheroid viability***

121 To dissect genetic dependencies of dormant ovarian cancer cells, we utilized a suspension
122 culture system that encourages cellular aggregation, leading to non-proliferative spheroids that
123 resemble dormant aggregates found in ovarian cancer patient ascites. **Fig. 1A** shows phospho-
124 western blots for ERK and p38 from three high grade serous EOC cell lines; iOvCa147,
125 OVCAR8, TOV1946. Reduced phospho-ERK and elevated phospho-p38 are indicative of the
126 characteristic signaling switch reported to underlie most paradigms of cancer cell dormancy (5).
127 To discover genes required for survival in spheroids, we utilized a new approach called GO-
128 CRISPR (Guide Only CRISPR) that we developed specifically for survival gene discovery in
129 three-dimensional organoid/spheroid cell culture conditions (**Fig. 1B**). GO-CRISPR incorporates
130 sgRNA abundances from non-Cas9-expressing cells to control for stochastic (non-Cas9
131 dependent) effects that are a challenge in three-dimensional culture conditions with slow or
132 arrested proliferation. We used sequencing to determine sgRNA identity and abundance in the
133 library, initially infected cells, and in cells following 48 hours of suspension culture (**Fig. 1B**).
134 Read count data was analyzed using a software package that we developed to analyze GO-
135 CRISPR data (summarized in **Sup. Fig. 1A&B**). We filtered the results for genes that had a
136 Spheroid/Adherent Enrichment Ratio (ER) less than 1, with a $P<0.05$, which is indicative of
137 genes that were most depleted in dormant suspension conditions (**Fig. 1B**). To assess reliability
138 of screen data, we investigated the classification of non-targeting control sgRNAs. We computed
139 a receiver operator characteristic curve (ROC) and determined the area under the curve for each
140 cell line (**Sup. Fig. 1C**). Greater than 95% of sgRNAs in iOVCA147 and OVCAR8 screens were
141 classified as non-essential, while 83% of sgRNAs in TOV1946 cells were non-essential. In

142 addition, we compared GO-CRISPR screen ER values with viability data from siRNA knock
143 down for 35 individual genes we have previously studied in spheroid survival assays (**Sup. Fig.**
144 **1D**)(16). This revealed a statistically significant correlation between the two sets of data,
145 suggesting that genes we previously knew supported spheroid viability (or were dispensable)
146 were classified similarly by our screen. These controls suggested our screen data was reliable for
147 identifying new survival dependencies.

148 We found 6,717 genes with an ER below 1 in iOvCa147 cells; and 7,637 genes in
149 TOV1946; and 7,640 genes in OVCAR8 cells. Among these genes; 1,382 were commonly
150 depleted in suspension culture in all three cell lines (**Fig. 1D**). We performed pathway
151 enrichment analysis on these common genes and identified several significantly enriched
152 pathways. These include primary Reactome gene sets such as signal transduction, metabolism,
153 and signaling by GPCR (**Fig. 1E**). In addition, we identified a tertiary category called 'axon
154 guidance,' that includes numerous components of the Netrin signaling pathway.

155

156 ***Expression of Netrin ligands and receptors are enriched in EOC spheroids***

157 DYRK1A was previously discovered to support survival of ovarian cancer cells in
158 suspension culture (16). Since DYRK1A phosphorylates RNA polymerase II in transcription
159 initiation (29), we sought to determine if it regulates gene expression in spheroid survival. We
160 created *DYRK1A*$^{-/-}$ iOvCa147 cells and confirmed their deficiency for survival in suspension
161 (**Sup. Fig. 2A-E**). Using iOvCa147 and *DYRK1A*$^{-/-}$ derivatives, we performed RNA-seq on
162 adherent and spheroid cells. We collected spheroids following a 6-hour incubation in suspension
163 because overexpression of known cell cycle transcriptional targets due to DYRK1A loss were

164 first evident at this time point, but loss of viability due to DYRK1A deficiency had not yet
165 occurred (16). We compared iOvCa147 adherent cells to 6-hour suspension culture to identify
166 transcriptional changes that occur as these cells transitioned from adherent conditions to
167 suspension conditions (**Fig. 2A**). We identified 1,834 genes that were upregulated, and pathway
168 enrichment analysis identified many of the same categories as our CRISPR screen including
169 axon guidance (**Fig. 2B**). We then compared iOvCa147 spheroid cells to *DYRK1A*$^{-/-}$ spheroid
170 cells to identify mRNA expression changes caused by DYRK1A deficiency (**Fig. 2C**). We
171 identified 744 genes that were downregulated and these also belonged to many of the same
172 pathways, including axon guidance (**Fig. 2D**).

173 We compared enriched pathways from these two RNA-seq analyses with those that were
174 identified in our GO-CRISPR screens to identify gene expression programs in spheroids whose
175 products are essential for cell survival. 78 Reactome pathways were commonly enriched across
176 the GO-CRISPR screens and transcriptomic analyses, including 78 of the 83 pathways identified
177 in RNA-seq from *DYRK1A*$^{-/-}$ spheroid cells (**Fig. 2E**). The axon guidance pathway was one of
178 the most enriched among these common pathways (**Fig. 2F**). These data reveal that our GO-
179 CRISPR screen and transcriptomic analyses converge on this highly specific tertiary Reactome
180 category of axon guidance alongside much broader primary or secondary gene sets. This
181 category includes Netrin ligands, receptors, and downstream signaling components, suggesting a
182 previously unappreciated role in HGSOC spheroid viability.

183 We separately sought to confirm expression of Netrins and their signaling components in
184 HGSOC spheroids. We examined expression levels of ligands and receptors in the three cell
185 lines used in our GO-CRISPR screen using RT- qPCR (**Fig. 3A-C**). The precise identities of
186 upregulated genes varies between cell lines, however each cell line increases expression of some

187 Netrins, at least one UNC5, and at least one of DCC, DSCAM, and Neogenin. This suggests that
188 the Netrin pathway may play a previously unappreciated role in HGSOC dormancy and disease
189 progression. Since Netrin signaling has not been previously reported in HGSOC dormancy we
190 examined expression of Netrin-1 and -3 ligands in spheroids isolated directly from patient ascites
191 by immunohistochemistry (**Fig. 3D-F**). We confirmed Netrin-1 and -3 antibody specificity using
192 spheroids generated from OVCAR8 cells bearing knock out or over expression of these Netrins
193 (**Sup. Fig. 3**). Spheroids were paraffin embedded and serial sections were also stained with
194 epithelial markers Cytokeratin and EpCAM, as well as p53 to confirm cancer cell identity within
195 spheroids that co-stain for Netrins (**Fig. 3D-F**). Overall, this confirms Netrin expression occurs
196 in HGSOC patient spheroids in precisely the context our screen indicates that it is critical for cell
197 survival.

198

199 ***Netrin signaling stimulates ERK to support HGSOC spheroid survival.***

200 Netrin ligands and their dependence receptors are best known for their roles in axon guidance
201 (30), but are appreciated to regulate apoptosis in cancer (19). **Fig. 4A** illustrates components of
202 Netrin signaling and the frequency with which they were discovered to have an ER of <1 in our
203 screens. In addition, intracellular signaling molecules known to be downstream of Netrin
204 receptors, and that are shared with other enriched pathways identified in our screens are also
205 illustrated. To confirm screen findings, we independently knocked out *NTN1*, *NTN3*, *NTN4*,
206 *NTN5*, the UNC5H receptor homologs (*UNC5A*, *UNC5B*, *UNC5C*, and *UNC5D*), as well as
207 *DCC*, *DSCAM*, and *NEO1* alone or in multigene combinations using lentiviral delivery of
208 sgRNAs and Cas9 (**Fig. 4B and Sup. Fig. 4**). We assessed their loss on spheroid survival in six
209 HGSOC cell lines (iOvCa147, TOV1946, OVCAR3, OVCAR4, OVCAR8, and COV318). Loss

210 of at least one netrin ligand resulted in reduced spheroid cell survival in five of six cell lines
211 (**Fig. 4B**). Notably, Netrin-3 loss showed the most pronounced effect on survival. Cell lines such
212 as OVCAR8 and COV318 were relatively resistant to the deletion of netrin pathway components
213 as individual UNC5H, *DCC*, and *DSCAM* genes rarely affected viability (**Fig. 4B**). In these
214 instances, combined deletions of UNC5H family members, or *DCC;DSCAM;NEO1* (DDN for
215 short) were either inviable or highly sensitive to suspension culture induced cell death suggesting
216 redundancy in this pathway in some cell lines. Other cell lines, such as OVCAR3, were highly
217 sensitive to the loss of multiple individual ligands and any individual UNC5H receptor was
218 highly sensitizing to death induction in suspension culture (**Fig. 4B**). Overall, these illustrate a
219 robust and redundant role for Netrins in survival in this dormant cell culture assay. Importantly,
220 loss of receptor expression does not elevate viability as expected for a dependence receptor,
221 suggesting that Netrin receptors in HGSOC simply transmit positive survival signals.

222 To determine if Netrin dependent signaling is active in EOC spheroids, we transferred
223 serum deprived adherent cells to suspension and stimulated with recombinant Netrin-1 (**Fig. 4C**).
224 Western blotting for phospho-ERK, as a measure of activation, reveals stimulation of MEK-ERK
225 signaling in each of the cell lines tested under spheroid culture conditions. Because MEK and
226 ERK family members were identified in our screens (**Fig. 4A**), Netrin is a candidate pathway to
227 provide low level, but essential survival signals through the MAPK pathway. We investigated
228 the dependence of ERK phosphorylation on UNC5H and DDN receptors and demonstrate it is
229 lower when receptors are deleted (**Fig. 4D**). Activation using Netrin-1 stimulation of suspension
230 cultures of OVCAR8 cells, or derivatives deleted for UNC5 family members or DDN receptors,
231 indicates that Netrin receptors are essential to activate ERK in dormant suspension culture (**Fig.
232 4E**). Inhibition of MEK using the MEK1/2 inhibitor PD184352 causes loss of cell viability in

233 suspension culture (**Fig. 4F**), emphasizing that MEK-ERK signaling is key to cell survival. The
234 simplest explanation of this data is that Netrins signal through a heterodimer or multi-receptor
235 complex containing both an UNC5 and DDN component that provides stimulation for MEK and
236 ERK in the absence of mitogenic signals in dormant culture conditions.

237 ***Netrin overexpression is correlated with poor outcome in HGSOC.***

238 Genomic studies indicate that HGSOC is one of the most aneuploid cancers (31). In
239 addition to the frequency of copy number variants per tumor, the locations of gains and losses
240 are dissimilar between cases, making this a highly heterogenous disease. Evaluation of TCGA
241 genomic data for HGSOC indicates rare amplifications or deletions of Netrin or Netrin-receptor
242 genes (**Sup. Fig. 5A**). Because of redundancy of Netrins and their receptor families this data
243 suggests HGSOC cases with deficiency for Netrin signaling are rare. This is consistent with our
244 data that all six cell lines tested reveal evidence of Netrin component dependence for survival
245 (**Fig. 4B**). Some TCGA HGSOC cases display elevated gene expression for Netrins or their
246 receptors, but only rare cases display low expression (**Sup. Fig. 5B**). Collectively, this suggests
247 that Netrin signaling in HGSOC is retained despite high copy number variation in this cancer
248 type and there is occasional overexpression.

249 In agreement with our experimental data that multiple Netrin ligands can contribute to
250 spheroid survival in HGSOC (**Fig. 4A&B**), sorting cases by high level expression of Netrin-1
251 and -3 ligands reveals a significantly shorter survival compared to cases with low level
252 expression and this trend is evident in the cases that only overexpress Netrin-3 (**Fig. 5A**). This
253 genomic data supports the interpretation that Netrin signaling is retained in HGSOC and its
254 elevation is deleterious to patient outcome.

255 We investigated overexpression of Netrin-1 and -3 in spheroid survival by generating
256 OVCAR8 derivatives that stably overexpress these proteins (**Fig. 5B**). We then utilized these
257 cells in suspension culture assays for spheroid survival as before (**Fig. 5C**). This data indicates
258 that overexpression of either Netrin-1 or -3 increases OVCAR8 cell survival in dormant spheroid
259 culture conditions. Examination of fixed spheroids isolated from this experiment further
260 indicates that elevated survival in this experiment is explained by an increase in abundance of
261 individual spheroids that overexpress either Netrin-1 or -3 (**Fig. 5D**). These experiments reveal
262 the significance of a previously undiscovered role for Netrins in HGSOC. High level expression
263 correlates with poor outcome and in suspension culture, overexpression confers oncogenic
264 properties on HGSOC cells.

265

266 ***Netrin overexpression induces abdominal spread of HGSOC.***

267 Our findings from CRISPR screens and cell culture experiments indicate that Netrin
268 signaling supports dormant HGSOC cell survival. Our analysis of TCGA is also predictive of a
269 worse outcome for patients. We sought to solidify these findings by searching for how Netrin
270 signaling affects HGSOC disease pathogenesis.

271 We utilized a xenograft assay in which OVCAR8 cells overexpressing Netrin-1 or -3
272 were injected into the peritoneal cavity and compared with OVCAR8 cells bearing an empty
273 vector as control. Mice were harvest following 35 days to analyze disease dissemination and
274 characterize the effect of Netrins in this model of HGSOC metastatic spread (**Fig. 6A**). Necropsy
275 of all animals at endpoint allowed for the identification and quantitation of tumor nodules within
276 the abdomen (**Fig. 6B**). Petal plots illustrate the frequency of specific organ and tissue sites

277 displaying tumor nodules (**Fig. 6B**). This revealed spread to the omentum was similar across all
278 genotypes of xenografted cells and occurred in all mice (**Fig. 6B**). In contrast, tumor nodules
279 were detected with increased abundance on the diaphragm, the liver, and mesenteries that
280 support the uterus (mesometrium) (**Fig. 6B**). In addition to more frequent disease spread to these
281 locations caused by Netrin overexpressing cells, we note that the quantity of nodules was also
282 increase in comparison with OVCAR8 control cells (**Fig. 6C-F**). We confirmed the source of
283 these lesions to be the xenografted cells using immunohistochemical staining for human
284 cytokeratin (**Fig. 6G,H**). Lastly, Netrin-1 and -3 histochemical staining confirms its presence in
285 the local tumor microenvironment (**Fig. 6G,H**). The similarity of increased tumor nodules seen
286 in xenografts and elevated spheroid formation and viability seen in culture suggests that Netrin
287 improve cell viability in spheroid aggregates in vivo leading to increased disease spread.

288 **Discussion**

289 In this report we investigated survival mechanisms in a model of HGSOC dormancy. We
290 utilized a modified CRISPR screening approach that was adapted to discover gene loss events in
291 largely non-proliferative conditions. We compared essential genes discovered in the screen with
292 gene expression increases identified by RNA-seq in dormant HGSOC cultures. This implicated
293 the Netrin signaling pathway in HGSOC spheroid survival. We independently validated the role
294 of Netrins, their receptors, and downstream intracellular targets MEK and ERK in the survival
295 biology of HGSOC cells in dormant culture. Furthermore, we reveal that overexpression of
296 Netrin-1 and -3 are correlated with poor clinical outcome in HGSOC and over expression of
297 these ligands induces elevated survival in dormant HGSOC culture conditions and disease spread
298 in a xenograft model of dissemination. Our work implicates Netrins, their receptors, and MEK-
299 ERK as a previously unappreciated, but critical signaling network in HGSOC survival.

300 HGSOC spheroid cell biology has presented a unique challenge to cancer chemotherapy.
301 Dormant spheroids are most abundant in patients with late-stage disease and they contribute to
302 therapeutic resistance and seed metastases (32-34). Hence, there is a critical unmet need to
303 understand HGSOC spheroid dependencies and target them therapeutically. Our data suggests
304 that Netrin signaling is a universally active mechanism in spheroid cell survival. HGSOC is
305 characterized by extensive genomic rearrangements and copy number variants (31), and we
306 speculate that Netrin signaling is retained because of the extensive redundancy of components of
307 this pathway. Netrin-1 and -3 can both contribute to survival signaling and knock out of three or
308 four different Netrin receptors is necessary to compromise Netrin signaling in survival. A key
309 goal for the future is to identify Netrin-1 or -3 overexpression patients and compare their specific
310 disease progression patterns with our xenograft model. This will be most informative of the

311 effects of Netrin ligand overexpression in scenarios of dormancy, metastasis, and chemotherapy
312 resistance.

313 This study demonstrates that Netrins function to stimulate UNC5H and fibronectin repeat
314 containing receptors such as DCC to activate survival signals in HGSOC spheroids. This is
315 distinct from the known role of UNC5H and DCC as dependence receptors where Netrin inhibits
316 their pro-apoptotic signaling (21). Our data does not show elevated survival of spheroid cells in
317 response to deletions of receptors, even in instances where families of Netrin receptors are co-
318 deleted. Consistent with this observation, over expression of Netrin-1 or -3 in OVCAR8 cells
319 stimulates higher level survival in suspension. In colon cancer, frequent deletions of DCC confer
320 a survival advantage and underscore the dependence receptor concept (35, 36). In HGSOC DCC
321 or UNC5H deletions are relatively rare (31). This suggests that ovarian cancer cells utilize Netrin
322 signals for positive survival signaling instead of to neutralize inherent death signals from
323 dependence receptors. Our data suggests that Netrin activates MEK and ERK to support cell
324 survival indicating that targeting ligands, receptors or downstream at MEK are all possible
325 approaches to inhibit this survival pathway. Netrin-1 inhibition in solid tumor xenograft models
326 of melanoma have been shown to be effective in combination with chemotherapy (37), but its
327 effects on a dormant scenario are unknown. Identifying agents that cooperate with standard
328 HGSOC chemotherapeutic agents such as carboplatin would offer an attractive strategy to
329 eradicate dormant cells while combating progressive disease. Alternatively, a novel approach to
330 targeting dormancy discovered in this study is, ironically, MEK inhibition. Dormancy is
331 characterized by low phospho-ERK levels (3, 6), indicating low MEK activity, yet low levels of
332 RAS-MAPK signaling are known to provide survival signals (38). A challenge with deploying
333 MEK inhibitors as an anti-dormancy setting in HGSOC therapy is its incompatibility with

334 standard chemotherapies that rely on cell proliferation. Overall, our study aimed to identify
335 potential new therapeutic targets in dormancy and Netrins and MEK are feasible new candidates
336 for dormant HGSOC disease.

337 Current literature offers little to connect Netrins with HGSOC beyond the observation
338 that *NTN1* expression is increased in tumors compared to benign lesions (39). Similarly, recent
339 dormancy literature beyond HGSOC does not include a role for Netrins (3-6, 40). We expect that
340 Netrin signaling may play an unappreciated role in dormancy in other cancer disease site
341 paradigms. As stated in the introduction, dormancy is characterized by acquisition of stem like
342 properties, EMT, and in most paradigms it involves rare cells establishing themselves in
343 perivascular or bone marrow niches. A chick chorioallantoic membrane assay of metastasis in
344 which MDA-MB-231 cells were seeded was monitored for lung dissemination. Inhibition of
345 Netrin-1 with NP137 and treatment with decitabine has been shown to reduce lung seeding
346 suggesting that Netrins are relevant in a metastatic scenario that may include dormant
347 intermediate steps in dissemination (41). Furthermore, Netrin signaling through UNC5B is
348 known to direct vascular branching (42). This suggests that Netrins are available in the
349 perivascular niche where dormant cells often reside. Lastly, Netrin-1 has been shown to be a
350 component of the bone marrow niche that suppresses hematopoietic stem cell proliferation (43).
351 While not a cancer dormancy scenario, it indicates that Netrins support some solitary dormant
352 cell properties and are expressed by resident cells in the appropriate dormant cell niches beyond
353 just HGSOC. For these reasons we expect Netrins will have a significant role in tumor dormancy
354 beyond ovarian cancer.

355 **Methods**

356 *Cell Lines and Engineering Cas9+ cells:* High-grade serous ovarian cancer (HGSOC) cell lines
357 OVCAR3, OVCAR4, OVCAR8, COV318, TOV1946 and iOvCa147 were used in this study.
358 The iOvCa147 cells have previously been characterized and reported (44). All cell lines were
359 verified by STR analysis. iOvCa147, OVCAR8, and TOV1946 cells were engineered to express
360 Cas9 using pLentiCas9-Blast and clones were isolated. High Cas9 editing efficiency was
361 determined by viability studies using sgRNAs targeting selected fitness genes (PSMD1, PSMD2,
362 EIF3D) and a non-targeting control (LacZ) as previously described (45).

363 *Lentiviral sgRNA library preparation:* HEK293T cells were transfected with the combined A
364 and B components of the GeCKO v2 whole genome library (123,411 sgRNAs in total) along
365 with plasmids encoding lentiviral packaging proteins (46). Media was collected 2-3 days later,
366 cells and debris were pelleted by centrifugation, and supernatant containing viral particles was
367 filtered through a 0.45 μM filter and stored at −80°C with 1.1 g/100 mL BSA.

368 *GO-CRISPR screens in iOvCa147, OVCAR8, and TOV1946 cells:* Cas9-positive and Cas9-
369 negative cells were separately transduced with lentiviruses at a multiplicity of infection of 0.3
370 and with a predicted library coverage of >1000-fold. Cells were selected in puromycin and
371 maintained in complete media (DMEM/F12 with 10% FBS, 1% pen-strep-glutamine), containing
372 puromycin in all following steps. More than 10^9 cells were collected and split into three groups
373 consisting of approximately 3.0×10^8 cells. Triplicate samples of 6.2×10^7 cells were saved for
374 sgRNA sequence quantitation (T_0). The remaining cells were seeded at 2.0×10^6 cells/mL in 20
375 x 10 cm ULA plates. Following 2 days of culture, media containing spheroids was transferred to
376 10 x 15 cm adherent tissue culture plates. The next day unattached spheroid cells were collected
377 and re-plated onto additional 15 cm plates. This process was repeated for a total of 5 days to

378 maximally capture viable cells. Attached cells were collected and pooled for DNA extraction
379 (T_f). Genomic DNA was extracted using the QIAmp DNA Blood Maxi Kit (Qiagen, #51194).
380 PCR amplification and barcoding was performed as described (Hart paper, Cell, 2015). Next
381 generation sequencing was performed using an Illumina MiSeq 50 cycle kit on an Illumina
382 MiSeq platform.

383 *TRACS analysis:* The library reference file containing a list of all sgRNAs and their sequences
384 (CSV file), raw reads for the pooled sgRNA library (FASTQ files (L0) and raw reads (FASTQ
385 files) for all T_0 and T_f timepoints and replicates for Cas9-positive and Cas9-negative cells were
386 loaded into TRACS (https://github.com/developerpiru/TRACS). TRACS then automatically
387 trimmed the reads using Cutadapt (v1.15), built a Bowtie2 (v2.3.4.1) index and aligned the reads
388 using Samtools (v1.7). TRACS used the MAGeCK read count function (v0.5.6) to generate read
389 counts and incremented all reads by 1 to prevent zero counts and division-by-zero errors. The
390 TRACS algorithm was then run using this read count file to determine the Library Enrichment
391 Score (ES), Initial ES, Final ES and the Enrichment Ratio (ER) for each gene. VisualizeTRACS
392 was used to generate graphs of Initial and Final ratios.

393 *Pathway enrichment analyses:* For GO-CRISPR screens and multi-omics comparisons, we used
394 the filtered list of genes obtained using TRACS and performed gene ontology and pathway
395 enrichment analysis using the ConsensusPathDB enrichment analysis test (Release 34
396 (15.01.2019), http://cpdb.molgen.mpg.de/) for top-ranked genes of interest. p_{adj} values and ER
397 values for each gene were used as inputs. The minimum required genes for enrichment was set to
398 45 and the FDR-corrected p_{adj} value cutoff was set to < 0.01. The Reactome pathway dataset was
399 used as the reference. For each identified pathway, ConsensusPathDB provides the number of

400 enriched genes and a q value (p_{adj}) for the enrichment. Bar plots were generated in R 3.6.2 using
401 these values to depict the significant pathways identified.

402 *Generating DYRK1A knockout cells:* A double cutting CRISPR/Cas9 approach with a pair of
403 sgRNAs (sgRNA A and B) was used to completely excise exon 2 (322 bp region) of *DYRK1A*
404 using a px458 vector (Addgene #48138) that was modified to express the full CMV promoter.
405 PCR primers that flank the targeted region of *DYRK1A* were used to verify deletion. Single-cell
406 clones were generated by liming dilutions and evaluated for DYRK1A status by PCR, western
407 blot, and sequencing. See Supplemental Table 1 for sgRNA and PCR primer sequences.

408 *DYRK1A IP kinase assay:* Whole cell lysates from adherent parental iOvCa147 cells and
409 *DYRK1A*$^{-/-}$ cells were extracted using complete RIPA buffer and incubated overnight with
410 DYRK1A antibody (Cell Signaling Technology anti-DYRK1A rabbit antibody #8765). Samples
411 were then washed with buffer and Dynabeads (Thermo Fisher Scientific Dynabeads Protein G
412 #10003D) were added for 2 hours. Samples were then washed with buffer and recombinant Tau
413 protein (Sigma recombinant Tau protein #T0576) and ATP (Sigma #A1852) were added and
414 samples were incubated for 30 minutes at 37°C. 5x SDS was then added and samples were
415 resolved by SDS-PAGE. Antibodies used for western blotting were phosphospecific Tau
416 antibody (Cell Signaling Technology phospho-Tau Ser-404 rabbit antibody #20194) and Tau
417 protein (Cell Signaling Technology anti-Tau rabbit antibody #46687).

418 *RNA preparation and RNA-sequencing:* Total RNA was collected from parental iOvCa147 cells
419 and *DYRK1A*$^{-/-}$ cells from 24-hour adherent or 6-hour spheroid conditions using the Monarch
420 Total RNA Miniprep Kit (NEB #T2010S) as described above. RNA was collected in three
421 replicates for each condition (adherent and spheroids). Samples were quantitated using Qubit 2.0
422 Fluorometer (Thermo Fisher Scientific) and quality control analysis using Agilent 2100

423 Bioanalyzer (Agilent Technologies #G2939BA) and RNA 6000 Nano Kit (Agilent Technologies
424 #5067-1511). Ribosomal RNA removal and library preparation was performed using ScriptSeq
425 Complete Gold Kit (Illumina #BEP1206). High-throughput sequencing was performed on an
426 Illumina NextSeq 500 platform (mid-output, 150-cyclekit).

427 *RNA-seq analyses:* Raw FASTQ data was downloaded from Illumina BaseSpace. Reads were
428 aligned using STAR 2.6.1a(47) to the human genome
429 (Homo_sapiens.GRCh38.dna.primary_assembly.fa; sjdbGTFfile:
430 Homo_sapiens.GRCh38.92.gtf) to generate read counts. DESeq2 was run with BEAVR(48) and
431 used to analyze read counts (settings: False discovery rate (FDR): 10%; drop genes with less
432 than 1 reads) to identify differentially expressed genes ($\log_2$ fold change > 1 for upregulated
433 genes; or $\log_2$ fold change < -1 for downregulated genes; $p_{adj} < 0.05$) for the following
434 comparisons: parental iOvCa147 adherent cells vs. parental iOvCa147 spheroid cells; or parental
435 iOvCa147 spheroid cells vs. *DYRK1A*$^{-/-}$ spheroid cells. For RNA-seq, we formed pathway
436 analyses in BEAVR and downloaded the pathway enrichment table to construct bar plots and
437 determine overlapping pathways using R 3.6.2.

438 *Western blots:* Adherent cells were washed in 1x PBS and lysed on the plate by the addition of
439 complete RIPA buffer with protease (Cell Signaling Technology #5871S) and phosphatase (Cell
440 Signaling Technologies #5870S) inhibitors and incubated for 5-10 minutes on ice. Spheres were
441 collected by gentle centrifugation at 300 rpm, washed gently in ice cold PBS, centrifuged again
442 and then resuspended in RIPA buffer as above. Samples were then centrifuged at 14,000 RPM at
443 4°C for 10 minutes. The supernatant liquid for each sample was collected and the pellets re-
444 extracted with RIPA containing the above inhibitor cocktails. Following centrifugation, the
445 supernates for each treatment were collected and pooled. Protein was determined by Bradford

446 assay. To assess the effect of Netrin 1 on downstream signaling, spheres incubated under non
447 adherent conditions for 5 days were challenged with the addition of 500 ng/ml human
448 recombinant Netrin-1 (R&D Systems #6419-N1-025) for a period of 20 minutes before collection.
449 Lysates were mixed with 6x SDS loading dye buffer and resolved using standard SDS-PAGE
450 protocols. Antibodies used for blotting were p42/44 MAPK (Erk1/2) (Cell Signaling Technology
451 rabbit antibody #4695), Phospho-p44/42 MAPK(Erk1/2) T202/Y204 (Cell Signaling
452 Technology; rabbit antibody #4370), p38 MAPK (Cell Signaling Technology; rabbit antibody
453 #9212), p38 MAPK T180/Y182 (Cell Signaling Technology; rabbit antibody #9211), DYRK1A
454 (Cell Signaling Technology anti-DYRK1A rabbit antibody #8765), Netrin-1 (Abcam rabbit
455 antibody #ab126729), Netrin-3 (Abcam rabbit antibody #ab185200), α-tubulin (Cell Signaling
456 Technology anti-αTubulin rabbit antibody #2125) and β-actin (Millipore Sigma rabbit antibody
457 #A2066).

458 *RT-qPCR analysis of gene expression:* Cells were triturated off the plate using Versene (0.5mM
459 EDTA in PBS), collected, counted and 10^6 cells plated onto Ultra-Low Attachment cell culture
460 dishes (Corning) to induce sphere formation. The spheres were collected after 24 h and RNA
461 extracted using the Monarch Total RNA Miniprep Kit (New England Biolabs #T2010S). RNA
462 was extracted from adherent cells directly from the plate. Extracted RNA was quantitated using a
463 NanoDrop and stored at -80° until used. First strand cDNA was generated from isolated RNA
464 using the iScript cDNA Synthesis Kit (Bio-Rad, #1708890) and RT-qPCR performed on the
465 resulting cDNA (diluted 5-fold) using the iQ SYBR Green Supermix (Bio-Rad, #1708882) and
466 following the manufactures instructions. Reactions were performed in 0.2ml non-skirted low
467 profile 96 well PCR plates (Thermo Scientifi, #AD-0700) using a CFX Connect Real Time
468 System thermo-cycler (Bio-Rad).

469 *TCGA patient data analyses:* We used the cBioPortal for Cancer Genomics
470 (https://www.cbioportal.org)(49) to analyze Netrin pathway alterations in Ovarian Serous
471 Cystadenocarcinoma patients (TCGA, PanCancer Atlas) for genomic alterations and mRNA
472 expression. OncoPrints were generated for mRNA expression (mean z-score threshold ± 1.5),
473 and mutations and putative copy number alterations for the following genes: *NTN1, NTN3,*
474 *NTN4, NTN5, UNC5A, UNC5B, UNC5C, UNC5D, DCC, DSCAM*. Survival analysis of *NTN1,*
475 and *-3* utilized patients from TCGA, PanCancer Atlas dataset and RNA-seq expression (high
476 expression z-score threshold > 1.2 and low is below 1.2).

477 *Generation of gene knockout cell lines:* Gibson Assembly (NEB #E2611) was used to clone
478 sgRNAs sequences derived from the GeCKO v2 library per gene of interest (*NTN1, NTN3,*
479 *NTN4, NTN5, DSCAM, DCC, NEO1, UNC5A, UNC5B, UNC5C, UNC5D,* and *EGFP* control
480 (See Supplemental Table 1 for sgRNA sequences for each)) into lentiCRISPR v2 (Addgene
481 #52961). For individual gene knockouts pooled libraries of up to four sgRNAs were generated.
482 For multiple gene knockouts pooled libraries of two sgRNAs/gene were constructed. To each 20-
483 nucleotide guide (Supplemental table I) was appended the 5' sequence, 5'-
484 TATCTTGTGGAAAGGACGAAACACC-3' and the 3' sequence, 5'-
485 GTTTTAGAGCTAGAAATAGCAAGTTAAAAT-3' (50). A 100 bp fragment was then
486 generated using the forward primer, 5'-
487 GGCTTTATATATCTTGTGGAAAGGACGAAACACCG-3', and reverse primer, 5'-
488 CTAGCCTTATTTTAACTTGCTATTTCTAGCTCTAAAAC-3′. The resulting fragment was
489 gel purified, quantitated by Qubit and cloned into the lentiviral vector as described (50). To
490 generate virus particles, HEK293T cells were transfected with the assembled plasmid along with
491 plasmids encoding lentiviral packaging proteins. Media was collected after 2-3 days and any

492 cells or debris were pelleted by centrifugation at 500 x g. Supernatant containing viral particles
493 was filtered through a low protein binding 0.45 μM filter. For each knockout, it was important to
494 ensure that each target cell was transduced with a full complement of guides. To ensure this, the
495 cells were transduced at relatively high MOI. Briefly, 25,000 cells were plated and transduced
496 with fresh HEK293T conditioned media containing virus. While we did not titer the viral
497 preparations for these experiments, previous experience indicated that we could generate
498 sufficiently high virus titers using our protocol. Under these conditions, we found a lack of
499 puromycin sensitive cells following 2-3 days in media containing 2-4 μg/ml puromycin
500 indicating that every cell received at least one virus particle. Multi-gene knock outs were created
501 through multiple rounds of infection with the relevant culture supernatants followed by one
502 round of puromycin selection.

503 *Generation of gene overexpression cell lines:* Plasmids encoding Netrin1 and Netrin3 were
504 obtained from Addgene (Ntn1-Fc-His, #72104 and Ntn3-Fc-His, #72105). Netrin1 was PCR
505 amplified using the forward primer 5'-
506 GCTATCGATATCCCAAACGCCACCATGATGCGCGCTGTGTGGGAGGCGCTG-3' and
507 reverse 5'-GCTATCTCTAGAGGCCTTCTTGCACTTGCCCTTCTTCTCCCG-3' and cloned
508 into the EcoRV/XbaI sites of pcDNA3.1/myc-HisA. For lentiviral expression, pcDNA NTN1
509 was amplified using the primers, forward 5'-
510 CACTGTAGATCTCCAAACGCCACCATGATGCGCGCTGTGTGGGAGGCGCTG-3' and,
511 reverse 5'-ACGCGTGAATTCTTATCAACCGGTATGCATATTCAGATCCTCTTCTGAGAT-
512 3' while NTN3 was amplified from pcDNA NTN3 using, forward 5'-
513 CTCGAGAGATCTGCGGCCGCCACCATGCCTGGCTGGCCCTGG-3' and the same reverse
514 primer as for NTN1. In this way both constructs carry a C-terminal Myc tag. Both cDNA's were

515 inserted into the BamHI/EcoRI sites of the lentiviral expression vector FUtdTW (Addgene
516 #22478). Construction of lentiviral particle and transduction into the target cells was as described
517 above. Selection was with Zeocin (ThermoFisher #R25001).

518 *Spheroid formation and reattachment assays:* For each targeted gene in iOvCa147, OVCAR3,
519 OVCAR4, OVCAR8, COV318, or TOV1946 cells, spheroid viability was assayed as follows:
520 Knockout cells were cultured for 72 hours in suspension conditions using ULA plasticware (2 ×
521 10^6 cells per well) to allow spheroid formation. Addition of therapeutics (PD184352) was made
522 at the time of plating. Spheroids were collected and transferred directly to standard plasticware to
523 facilitate reattachment for 24 hours. Reattached cells were fixed in 25% methanol in PBS for 3
524 minutes. Fixed cells were incubated for 30 minutes with shaking in 0.5% crystal violet, 25%
525 methanol in PBS. Plates were carefully immersed in water to remove residual crystal violet and
526 destained in 10% acetic acid in 1x PBS for 1 hour with shaking to extract crystal violet from
527 cells. Absorbance of crystal violet was measured at 590 nm using a microplate reader (Perkin
528 Elmer Wallac 1420). Each knockout was normalized to the EGFP control. Because crystal violet
529 binds protein, a linear relationship between the absorbance and the number of cells present is
530 obtained and may be represented as the percent of spheroid cells surviving suspension.

531 *Xenografts:* Female NOD-SCID mice were purchased from JAX (#001303). They were
532 engrafted between six and eight weeks of age with 4 x10^6 OVCAR8 control or modified
533 derivatives. Mice were housed for 35 days and euthanized and subjected to a necropsy to analyze
534 disease spread. Tumor lesions were photographed and quantitated. Abdominal organs and
535 associated tumor lesions were fixed in 10% formalin overnight and transferred to 70% ethanol
536 until embedded.

537 *Patient derived spheroids:* Patient derived spheroids were isolated from ascites fluid obtained
538 from debulking surgical procedures. These HGSOC samples were obtained with permission and
539 institutional REB oversight. Spheroids were prepared by filtering the ascites fluid through a
540 100μm mesh filter and washing the captured spheroids from the filter with PBS. The spheres
541 were collected by gravity on ice in PBS, washed twice with ice cold PBS and allowed to settle on
542 ice. Spheres were then fixed for 20 minutes in 10% formalin, washed, and resuspended in PBS
543 before being embedded in paraffin.

544 *Histology and immunohistochemistry:* Fixed organs from xenografts or spheroids were
545 embedded in paraffin, sectioned, and stained with H&E. Sections were deparaffinized by
546 standard procedures and antigen retrieval was performed in 10mM citrate, pH6.0. The sections
547 were blocked with 10% goat serum/3% BSA/0.3% Triton X-100 and stained with antibodies to
548 Netrin-1 (Abcam #ab126729, 1:200), Cytokeratin (human specific cytokeratin 7 and 8, ZETA
549 Corporation #Z2018ML, 1:200), EpCAM (Cell Signaling Technologies, #14452), p53 (Cell
550 Signaling Technologies, #2527) and Netrin-3 (1:250). Netrin-3 antibodies were generated using
551 immunized rabbits and their generation and purification will be published elsewhere. Primary
552 antibodies were followed with a biotinylated anti-rabbit (Vector Labs, # BA-1000) or anti-mouse
553 (Jackson ImmunoResearch, #115-067-003) IgG as a secondary antibody (1:500). Proteins were
554 visualized using DAB chemistry (ImmPACT DAB, Vector Labs, #SK-4105).

555 *Statistical analyses:* Specific statistical tests used are indicated in the figure legends for each
556 experiment. Analysis was done using GraphPad Prism 6.

557 **References**

558 1. Giancotti FG. Mechanisms governing metastatic dormancy and reactivation. Cell.
559 2013;155(4):750-64.
560 2. Massague J, Ganesh K. Metastasis-Initiating Cells and Ecosystems. Cancer Discov.
561 2021;11(4):971-94.
562 3. Sosa MS, Bragado P, Aguirre-Ghiso JA. Mechanisms of disseminated cancer cell
563 dormancy: an awakening field. Nat Rev Cancer. 2014;14(9):611-22.
564 4. Phan TG, Croucher PI. The dormant cancer cell life cycle. Nat Rev Cancer.
565 2020;20(7):398-411.
566 5. Goddard ET, Bozic I, Riddell SR, Ghajar CM. Dormant tumour cells, their niches and the
567 influence of immunity. Nat Cell Biol. 2018;20(11):1240-9.
568 6. Yeh AC, Ramaswamy S. Mechanisms of Cancer Cell Dormancy--Another Hallmark of
569 Cancer? Cancer Res. 2015;75(23):5014-22.
570 7. Lengyel E, Burdette JE, Kenny HA, Matei D, Pilrose J, Haluska P, et al. Epithelial
571 ovarian cancer experimental models. Oncogene. 2014;33(28):3619-33.
572 8. Lheureux S, Gourley C, Vergote I, Oza AM. Epithelial ovarian cancer. Lancet.
573 2019;393(10177):1240-53.
574 9. Lengyel E. Ovarian cancer development and metastasis. Am J Pathol. 2010;177(3):1053-
575 64.
576 10. Bowtell DD, Bohm S, Ahmed AA, Aspuria PJ, Bast RC, Jr., Beral V, et al. Rethinking
577 ovarian cancer II: reducing mortality from high-grade serous ovarian cancer. Nat Rev Cancer.
578 2015;15(11):668-79.
579 11. Shepherd TG, Dick FA. Principles of dormancy evident in high-grade serous ovarian
580 cancer. Cell Div. 2022;17(1):2.
581 12. Peart T, Ramos Valdes Y, Correa RJ, Fazio E, Bertrand M, McGee J, et al. Intact LKB1
582 activity is required for survival of dormant ovarian cancer spheroids. Oncotarget.
583 2015;6(26):22424-38.
584 13. Buensuceso A, Ramos-Valdes Y, DiMattia GE, Shepherd TG. AMPK-Independent
585 LKB1 Activity Is Required for Efficient Epithelial Ovarian Cancer Metastasis. Mol Cancer Res.
586 2019.
587 14. Chen MW, Yang ST, Chien MH, Hua KT, Wu CJ, Hsiao SM, et al. The STAT3-miRNA-
588 92-Wnt Signaling Pathway Regulates Spheroid Formation and Malignant Progression in Ovarian
589 Cancer. Cancer Res. 2017;77(8):1955-67.
590 15. Diaz Osterman CJ, Ozmadenci D, Kleinschmidt EG, Taylor KN, Barrie AM, Jiang S, et
591 al. FAK activity sustains intrinsic and acquired ovarian cancer resistance to platinum
592 chemotherapy. Elife. 2019;8.
593 16. MacDonald J, Ramos-Valdes Y, Perampalam P, Litovchick L, DiMattia GE, Dick FA. A
594 Systematic Analysis of Negative Growth Control Implicates the DREAM Complex in Cancer
595 Cell Dormancy. Mol Cancer Res. 2017;15(4):371-81.
596 17. Rajasekharan S, Kennedy TE. The netrin protein family. Genome Biol. 2009;10(9):239.
597 18. Kryza D, Wischhusen J, Richaud M, Hervieu M, Sidi Boumedine J, Delcros JG, et al.
598 From netrin-1-targeted SPECT/CT to internal radiotherapy for management of advanced solid
599 tumors. EMBO Mol Med. 2023;15(4):e16732.
600 19. Mehlen P, Delloye-Bourgeois C, Chedotal A. Novel roles for Slits and netrins: axon
601 guidance cues as anticancer targets? Nat Rev Cancer. 2011;11(3):188-97.

602 20. Arakawa H. Netrin-1 and its receptors in tumorigenesis. Nat Rev Cancer.
603 2004;4(12):978-87.
604 21. Brisset M, Grandin M, Bernet A, Mehlen P, Hollande F. Dependence receptors: new
605 targets for cancer therapy. EMBO Mol Med. 2021;13(11):e14495.
606 22. Forcet C, Stein E, Pays L, Corset V, Llambi F, Tessier-Lavigne M, et al. Netrin-1-
607 mediated axon outgrowth requires deleted in colorectal cancer-dependent MAPK activation.
608 Nature. 2002;417(6887):443-7.
609 23. Larrieu-Lahargue F, Welm AL, Thomas KR, Li DY. Netrin-4 induces lymphangiogenesis
610 in vivo. Blood. 2010;115(26):5418-26.
611 24. Yin K, Wang L, Zhang X, He Z, Xia Y, Xu J, et al. Netrin-1 promotes gastric cancer cell
612 proliferation and invasion via the receptor neogenin through PI3K/AKT signaling pathway.
613 Oncotarget. 2017;8(31):51177-89.
614 25. Llambi F, Lourenco FC, Gozuacik D, Guix C, Pays L, Del Rio G, et al. The dependence
615 receptor UNC5H2 mediates apoptosis through DAP-kinase. EMBO J. 2005;24(6):1192-201.
616 26. Castets M, Coissieux MM, Delloye-Bourgeois C, Bernard L, Delcros JG, Bernet A, et al.
617 Inhibition of endothelial cell apoptosis by netrin-1 during angiogenesis. Dev Cell.
618 2009;16(4):614-20.
619 27. Bruikman CS, Zhang H, Kemper AM, van Gils JM. Netrin Family: Role for Protein
620 Isoforms in Cancer. J Nucleic Acids. 2019;2019:3947123.
621 28. Jiang S, Richaud M, Vieugue P, Rama N, Delcros JG, Siouda M, et al. Targeting netrin-3
622 in small cell lung cancer and neuroblastoma. EMBO Mol Med. 2021;13(4):e12878.
623 29. Di Vona C, Bezdan D, Islam AB, Salichs E, Lopez-Bigas N, Ossowski S, et al.
624 Chromatin-wide profiling of DYRK1A reveals a role as a gene-specific RNA polymerase II
625 CTD kinase. Mol Cell. 2015;57(3):506-20.
626 30. Meijers R, Smock RG, Zhang Y, Wang JH. Netrin Synergizes Signaling and Adhesion
627 through DCC. Trends Biochem Sci. 2020;45(1):6-12.
628 31. Network CGA. Integrated genomic analyses of ovarian carcinoma. Nature.
629 2011;474(7353):609-15.
630 32. Ahmed N, Stenvers KL. Getting to know ovarian cancer ascites: opportunities for
631 targeted therapy-based translational research. Front Oncol. 2013;3:256.
632 33. Narod S. Can advanced-stage ovarian cancer be cured? Nat Rev Clin Oncol.
633 2016;13(4):255-61.
634 34. Keyvani V, Farshchian M, Esmaeili SA, Yari H, Moghbeli M, Nezhad SK, et al. Ovarian
635 cancer stem cells and targeted therapy. J Ovarian Res. 2019;12(1):120.
636 35. Fearon ER, Cho KR, Nigro JM, Kern SE, Simons JW, Ruppert JM, et al. Identification of
637 a chromosome 18q gene that is altered in colorectal cancers. Science. 1990;247(4938):49-56.
638 36. Mehlen P, Rabizadeh S, Snipas SJ, Assa-Munt N, Salvesen GS, Bredesen DE. The DCC
639 gene product induces apoptosis by a mechanism requiring receptor proteolysis. Nature.
640 1998;395(6704):801-4.
641 37. Boussouar A, Tortereau A, Manceau A, Paradisi A, Gadot N, Vial J, et al. Netrin-1 and
642 Its Receptor DCC Are Causally Implicated in Melanoma Progression. Cancer Res.
643 2020;80(4):747-56.
644 38. Downward J. Targeting RAS signalling pathways in cancer therapy. Nat Rev Cancer.
645 2003;3(1):11-22.
646 39. Papanastasiou AD, Pampalakis G, Katsaros D, Sotiropoulou G. Netrin-1 overexpression
647 is predictive of ovarian malignancies. Oncotarget. 2011;2(5):363-7.

648 40. Recasens A, Munoz L. Targeting Cancer Cell Dormancy. Trends Pharmacol Sci.
649 2019;40(2):128-41.
650 41. Grandin M, Meier M, Delcros JG, Nikodemus D, Reuten R, Patel TR, et al. Structural
651 Decoding of the Netrin-1/UNC5 Interaction and its Therapeutical Implications in Cancers.
652 Cancer Cell. 2016;29(2):173-85.
653 42. Lu X, Le Noble F, Yuan L, Jiang Q, De Lafarge B, Sugiyama D, et al. The netrin
654 receptor UNC5B mediates guidance events controlling morphogenesis of the vascular system.
655 Nature. 2004;432(7014):179-86.
656 43. Renders S, Svendsen AF, Panten J, Rama N, Maryanovich M, Sommerkamp P, et al.
657 Niche derived netrin-1 regulates hematopoietic stem cell dormancy via its receptor neogenin-1.
658 Nat Commun. 2021;12(1):608.
659 44. Tong JG, Valdes YR, Sivapragasam M, Barrett JW, Bell JC, Stojdl D, et al. Spatial and
660 temporal epithelial ovarian cancer cell heterogeneity impacts Maraba virus oncolytic potential.
661 BMC Cancer. 2017;17(1):594.
662 45. Hart T, Chandrashekhar M, Aregger M, Steinhart Z, Brown KR, MacLeod G, et al. High-
663 Resolution CRISPR Screens Reveal Fitness Genes and Genotype-Specific Cancer Liabilities.
664 Cell. 2015;163(6):1515-26.
665 46. Sanjana NE, Shalem O, Zhang F. Improved vectors and genome-wide libraries for
666 CRISPR screening. Nat Methods. 2014;11(8):783-4.
667 47. Dobin A, Davis CA, Schlesinger F, Drenkow J, Zaleski C, Jha S, et al. STAR: ultrafast
668 universal RNA-seq aligner. Bioinformatics. 2013;29(1):15-21.
669 48. Perampalam P, Dick FA. BEAVR: a browser-based tool for the exploration and
670 visualization of RNA-seq data. BMC Bioinformatics. 2020;21(1):221.
671 49. Cerami E, Gao J, Dogrusoz U, Gross BE, Sumer SO, Aksoy BA, et al. The cBio cancer
672 genomics portal: an open platform for exploring multidimensional cancer genomics data. Cancer
673 Discov. 2012;2(5):401-4.
674 50. Wang T, Lander ES, Sabatini DM. Large-Scale Single Guide RNA Library Construction
675 and Use for CRISPR-Cas9-Based Genetic Screens. Cold Spring Harb Protoc. 2016;2016(3):pdb
676 top086892.

677

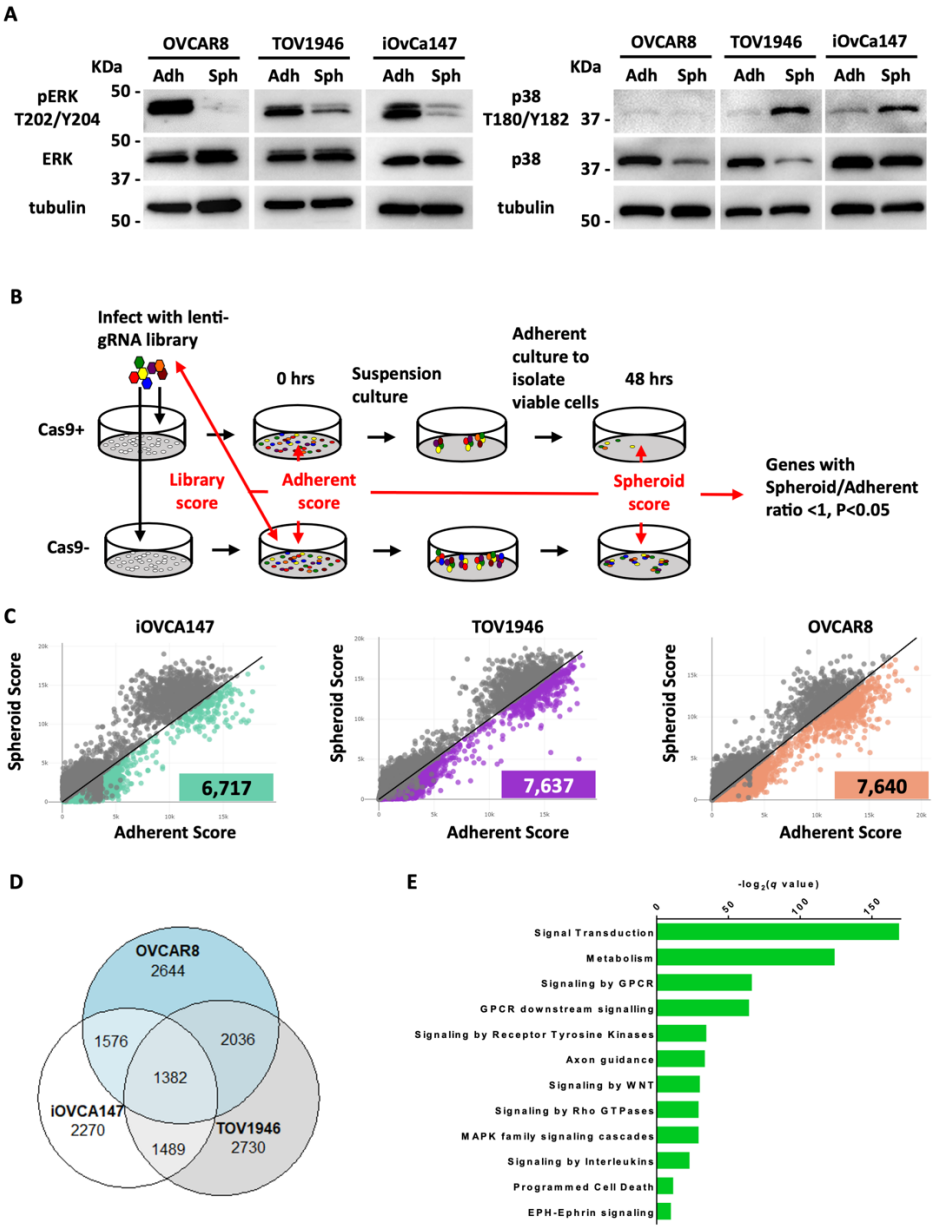

Figure 1. GO-CRISPR screens implicate axon guidance pathways as supporting EOC spheroid cell viability. **A)** iOvCa147, TOV1946, or OVCAR8 cells were cultured under adherent conditions (Adh) or in suspension to induce spheroids (Sph). Lysates were prepared and analyzed by western blotting for phosphorylated and total levels of ERK and p38. **B)** Flow chart of GO-CRISPR screening used for each of iOvCa147, TOV1946, or OVCAR8 control cells or that express Cas9. Cas9-positive cells (top row) and Cas9-negative cells (bottom row) were transduced with the GeCKO v2 pooled sgRNA library. After antibiotic selection, cells were expanded under adherent culture conditions (T_0) before being transferred to suspension culture conditions to induce spheroid formation and select for cell survival. After 48 hours spheroids were transferred to standard plasticware to isolate viable cells (T_f). Red arrows indicate the relevant comparisons of sgRNA sequence abundance that were made to analyze screen outcomes. **C)** Scatter plots representing spheroid score (T_f) on y-axis and adherent (T_0) score on x-axis calculated by TRACS for each gene in each cell line (iOvCa147, TOV1946, OVCAR8). Colored data points represent genes with ER < 1 and $p_{adj} < 0.05$. **D)** Venn diagram illustrating overlap of genes identified as supporting cell viability in suspension culture from iOvCa147, TOV1946, and OVCAR8 cells. **E)** Graph depicting enriched pathways from ConsensusPathDB using the 1382 commonly identified genes from D. Categories are ranked by q-value.

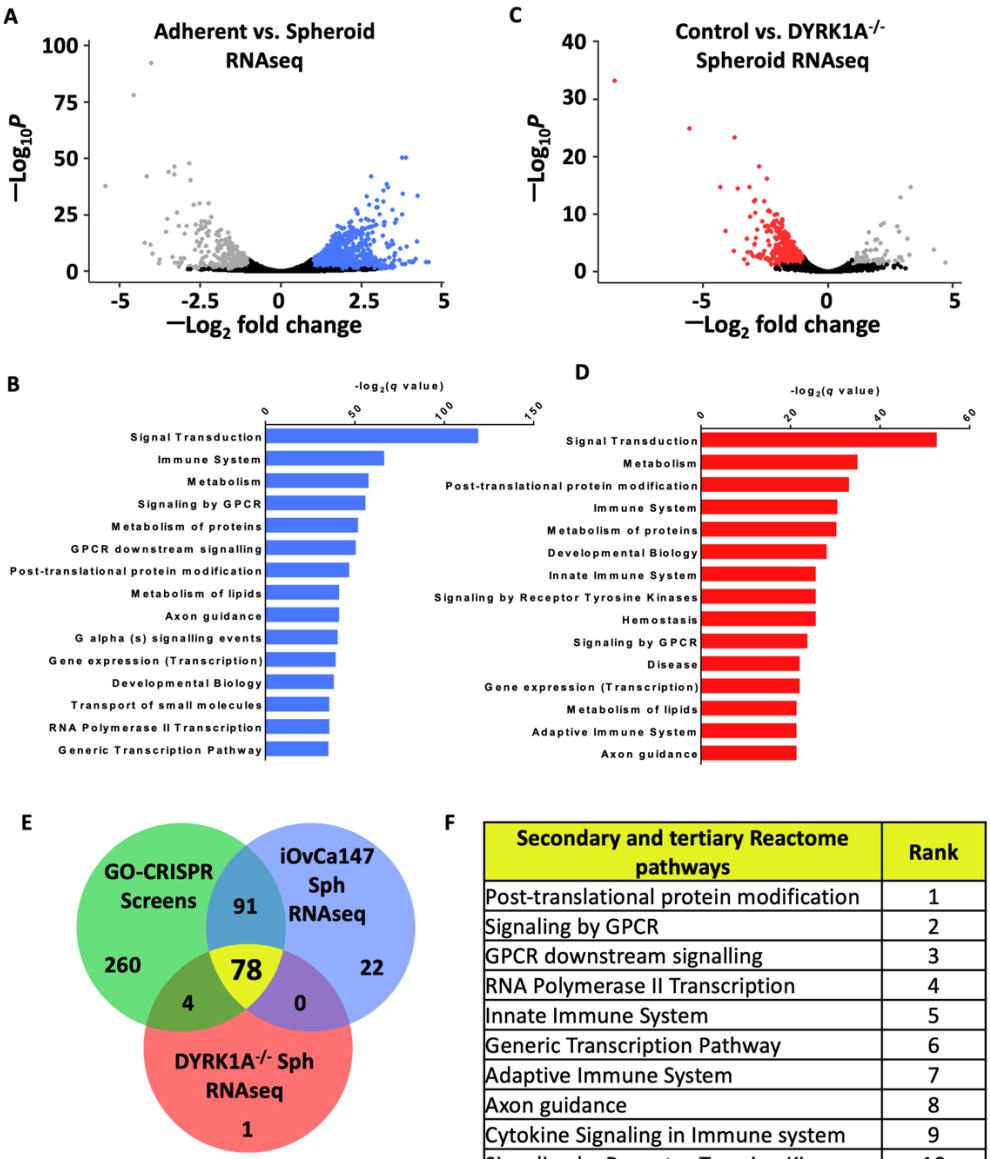

Secondary and tertiary Reactome pathways	Rank
Post-translational protein modification	1
Signaling by GPCR	2
GPCR downstream signalling	3
RNA Polymerase II Transcription	4
Innate Immune System	5
Generic Transcription Pathway	6
Adaptive Immune System	7
Axon guidance	8
Cytokine Signaling in Immune system	9
Signaling by Receptor Tyrosine Kinases	10

Figure 2. Axon guidance pathway components are upregulated in iOvCa147 spheroid cells in a DYRK1A dependent manner. A) RNA was isolated from iOvCa147 cells following culture under adherent conditions or in suspension conditions to induce spheroid formation for 6 hours. Triplicate independent cultures were processed for RNA-seq. A volcano plot shows differentially expressed genes in spheroid cells compared to adherent. 1,937 genes were found to be downregulated in iOvCa147 spheroid cells ($\log_2$ fold change < 1, $p_{adj} < 0.05$, FDR 10%, highlighted in grey) and 1,834 genes were upregulated ($\log_2$ fold change > 1, $p_{adj} < 0.05$, FDR 10%, highlighted in blue). **B)** Top 15 most significantly enriched pathways ($p_{adj} < 0.05$) whose genes were upregulated in suspension culture compared to adherent in RNA-seq analysis. **C)** A volcano plot showing differentially expressed genes in *DYRK1A*$^{-/-}$ spheroid cells compared to iOvCa147 spheroid cells. 744 genes were found to be downregulated in *DYRK1A*$^{-/-}$ spheroid cells ($\log_2$ fold change < 1, $p_{adj} < 0.05$, FDR 10%, highlighted in red) and 96 genes were upregulated ($\log_2$ fold change > 1, $p_{adj} < 0.05$, FDR 10%, highlighted in grey). **D)** Top 15 most significantly enriched pathways ($p_{adj} < 0.05$) that were represented by downregulated genes in DYRK1A-/- suspension culture compared to control cells in suspension. **E)** Venn diagram depicting overlapping enriched pathways identified in GO-CRISPR screens in green; enriched pathways identified in upregulated genes in parental iOvCa147 spheroid cells in blue; and enriched pathways identified in downregulated genes in *DYRK1A*$^{-/-}$ spheroid cells in red. 78 pathways were commonly enriched in all three datasets (shown in yellow). **F)** Top 10 most significantly enriched pathways ($p_{adj} < 0.05$) among the 78 identified in C.

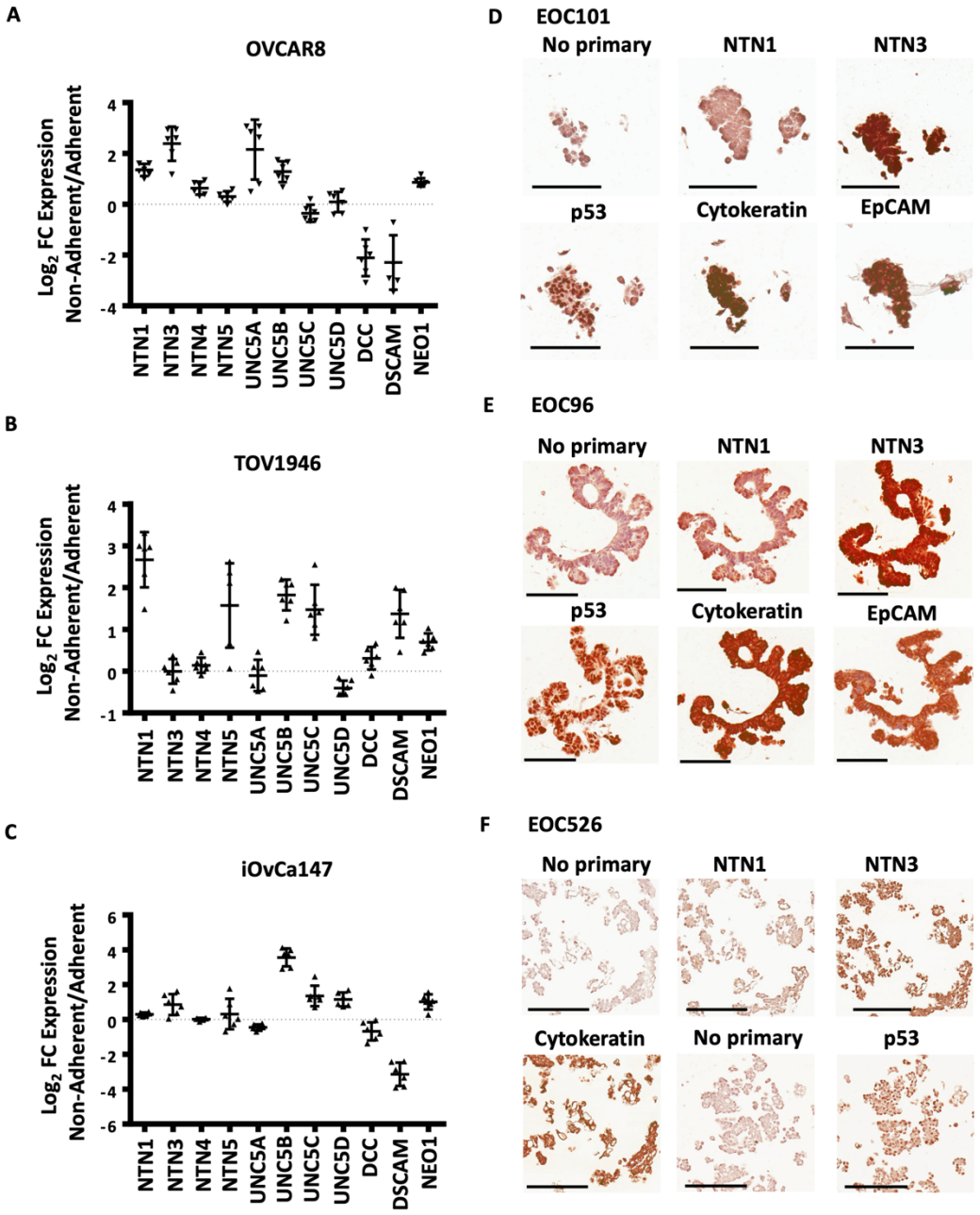

Figure 3. Expression of Netrin ligands and their dependence receptors is increased in suspension culture. A-C) RT-qPCR was performed to quantitate mRNA expression levels of Netrin ligands and receptors in three different HGSOC cell lines. Relative expression of the indicated transcripts is shown for suspension culture conditions. All experiments for performed in at least triplicate replicates. **D-F)**. Immunohistochemical staining was performed for the indicated proteins using spheroids isolated from HGSOC patient ascites that was fixed and paraffin embedded. Omission of primary antibody was used a control for background staining for each patient sample. Scale bar = 100µm

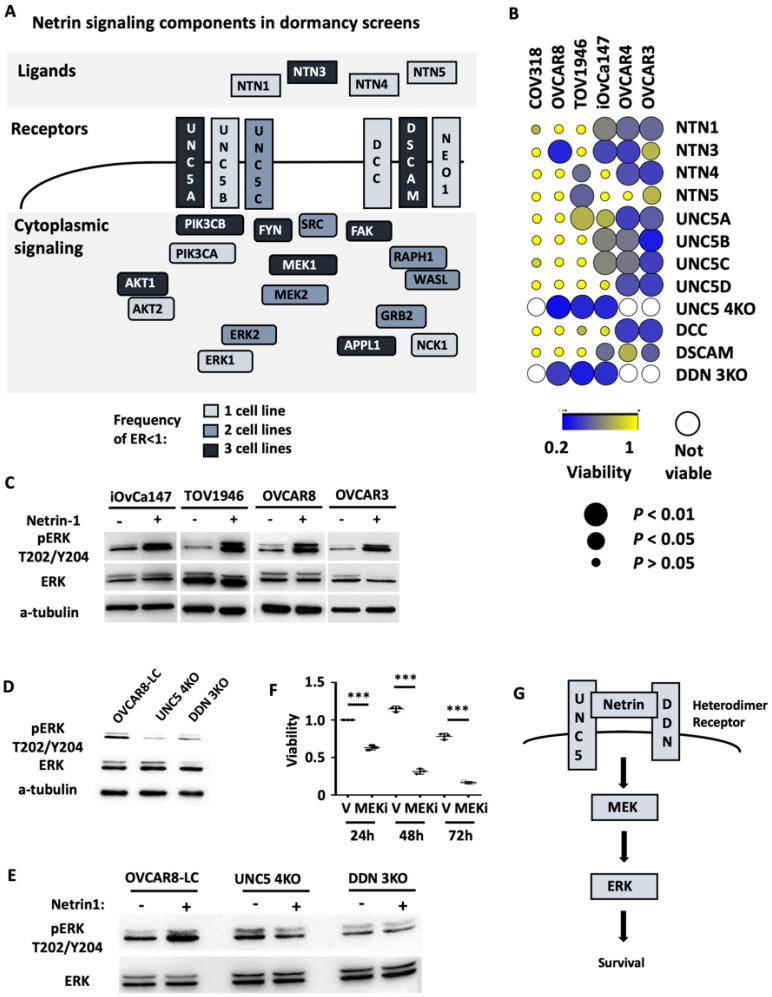

Figure 4. Netrin ligands and their receptors are required for spheroid cell survival. A) Illustration of netrin ligands, receptors, and other intracellular signaling molecules that are included in the Axon Guidance pathway category. The frequency of their identification in CRISPR screens is illustrated by shading and indicates how many cell lines had a negative enrichment ratio for a given component. **B)** The indicated ovarian cancer cell lines were infected with lentiviruses expressing sgRNAs directed against the indicated Netrin signaling genes. Cells were transferred to suspension culture conditions to induce spheroid formation for 72 hours and then returned to adherent conditions for 24 hours to facilitate reattachment. Re-attached cells were stained with Crystal Violet and retained dye was extracted and quantitated to measure relative survival. Each cell-gene combination was assayed in at least three biological replicates, averaged, and viability is displayed as a bubble plot. Mean survival for a given cell-gene combination was compared with GFP control gRNA transduced cells using anova and significance levels are illustrated by bubble size. Inviable cell-gene combinations are depicted as empty white spaces. **C)** Cultures of the indicated cell lines were serum starved and transferred to suspension culture conditions and stimulated. Netrin-1 signaling was analyzed by SDS-PAGE and western blotting for phospho-ERK, ERK, and tubulin. **D)** Suspension cultures of OVCAR8, or knock out derivatives, were harvested and analyzed for relative phosphorylation levels of ERK by western blotting. Total ERK and Tubulin blotting serves as expression and loading controls. **E)** Netrin-1 signaling in OVCAR8 cells deleted for all UNC5 receptors (UNC5 4KO) was tested by serum starving cells, transferring them to suspension, and stimulating with Netrin-1 as before. Western blotting for phospho-ERK, ERK, and tubulin were as before. **F)** OVCAR8 cells were seeded in suspension culture and treated with the MEK inhibitor PD184352 (PD) or DMSO vehicle for up to 72 hours. Mean viability was compared by anova (***P<0.005). **G)** Model summarizing the roles of Netrin ligands, receptors, and downstream targets MEK and ERK in dormant survival signaling.

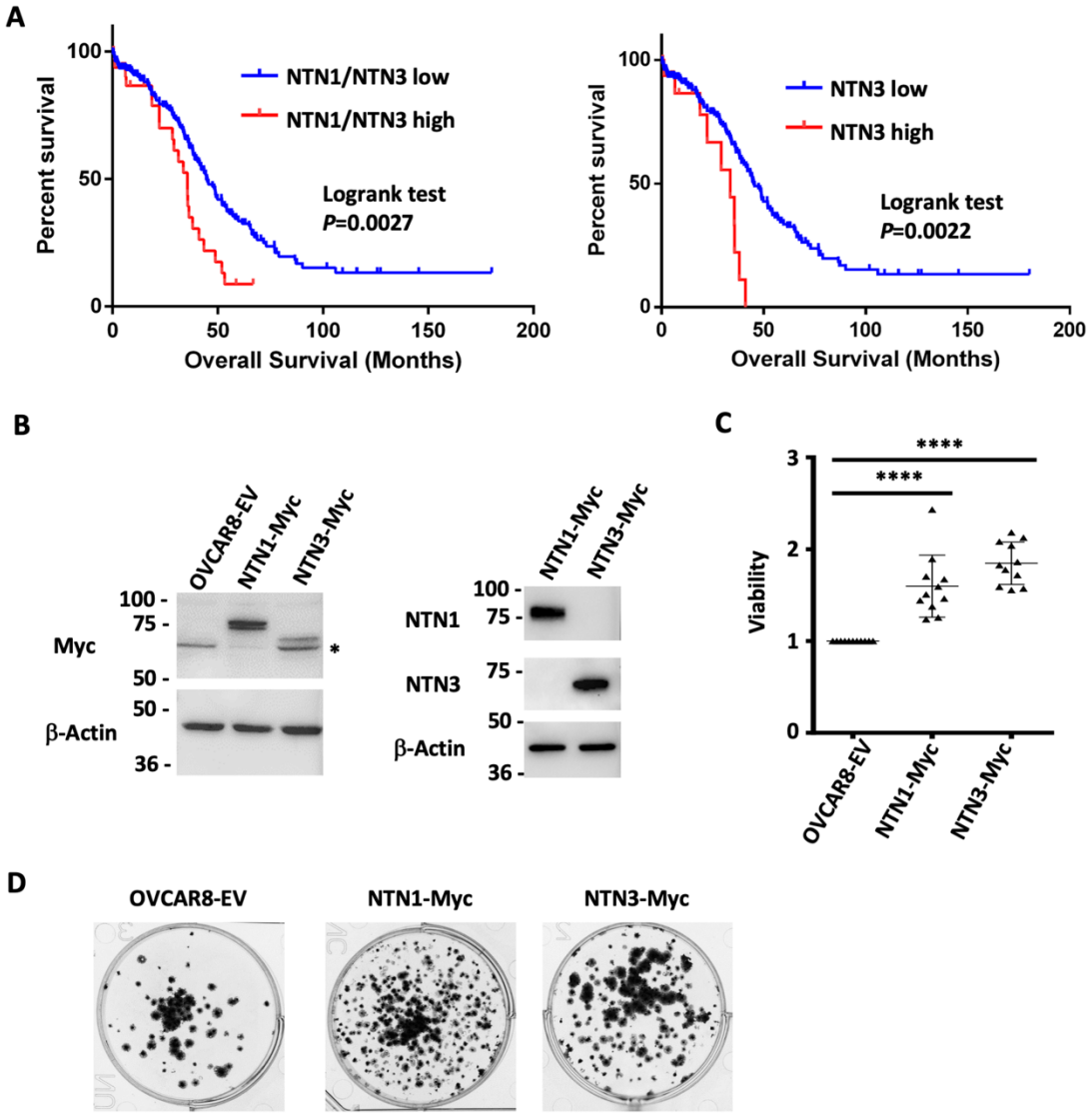

Figure 5. Netrin ligand overexpression is associated with poor clinical outcome in HGSOC. A) TCGA RNA-seq data for HGSOC patients (TCGA PanCancer Atlas study) was used to identify high Netrin-1 or -3 and low Netrin-1 or -3 expressing patients (high expressing are above z-score 1.2 and low are below 1.2). Overall survival was used to construct Kaplan-Meier plots and survival was compared using a logrank test. **B)** OVCAR8 cells were stably transduced with lentiviral constructs to overexpress epitope tagged Netrin-1 or -3. Western blotting for Netrins, Myc-tags, and tubulin were used to determine relative expression levels of both Netrins in these cell populations and vector controls. **C)** Control and Netrin overexpressing cells were transferred to suspension culture conditions to form spheroids, and replated to assay for viability. Mean viability and standard deviation is shown for each. Anova was used to compare survival (* P<0.05, *** P<0.001). **D)** Reattached spheroids were fixed and stained with Crystal Violet to examine size and abundance in control and Netrin-1 or -3 overexpression.

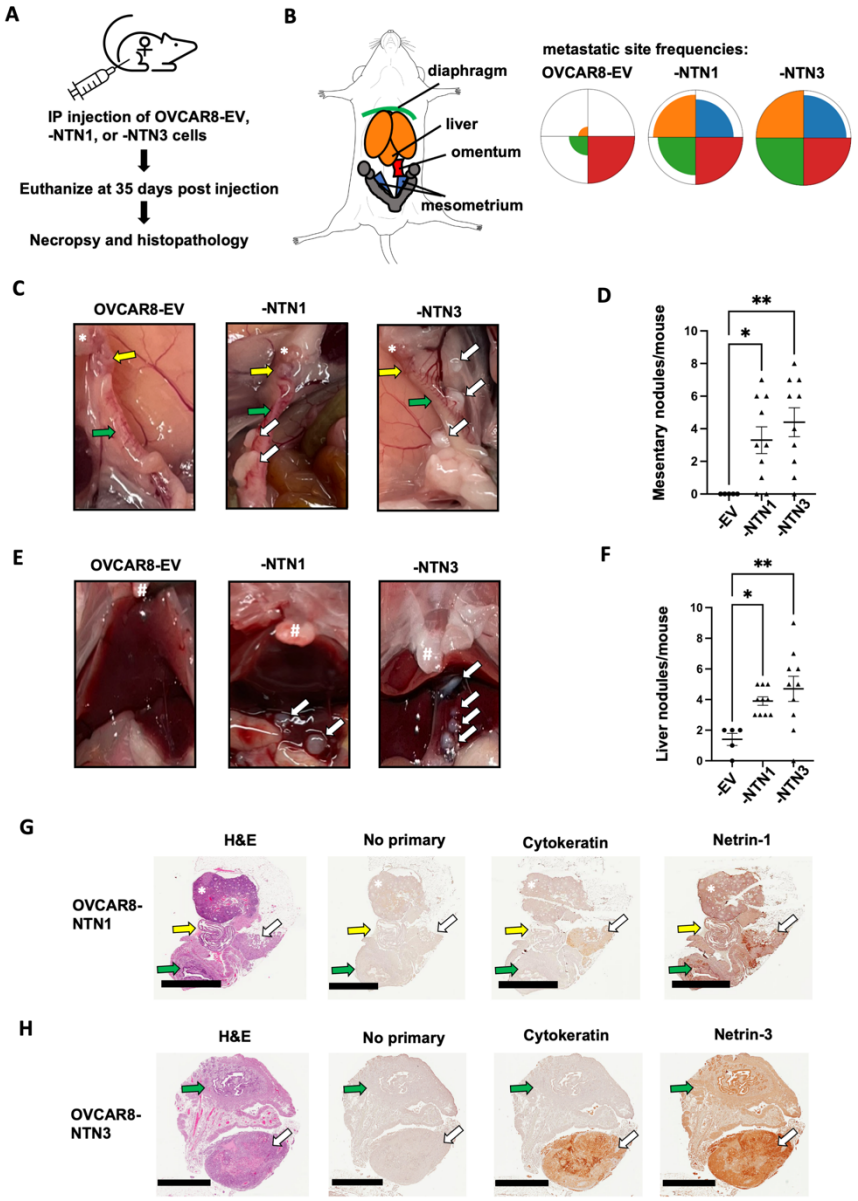

Figure 6. Netrin overexpression causes increased dissemination of tumor nodels. A) Netrin overexpressing and control OVCAR8 cells were injected into the intraperitoneal space of female NOD/SCID mice. Mice were euthanized following 35 days and analyzed for disease burden by necropsy and histopathology. **B)** The spread of cancer to the diaphragm, liver, omentum, and mesometrium was determined from necropsies and colors used in the anatomical schematic correspond with petal plots for each genotype of cells. Petal plots illustrate frequency of mice bearing disease spread to a particular location. The radius of color fill is proportional to the total number of animals with tumor nodules found in that location. **C)** Photographs of necropsy findings in the mesometrium. Locations of ovaries (*), oviduct (yellow arrow), and uterine horn (green arrow) are indicated in each case. Tumor nodules are indicated by white arrows. **D)** The number of mesometrium associated tumor nodules was determined for each mouse. Mean values are indicated and differences between genotype were determined by anova (* $P<0.05$, ** $P<0.01$). **E)** Photographs of necropsy findings in the liver. Location of sternum is indicated (#) in each image. Tumor nodules are indicated by white arrows. **F)** The number of liver associated tumor nodules was determined for each mouse. Mean values are indicated and differences between genotype were determined by anova (* $P<0.05$, ** $P<0.01$). **G** and **H)** Histology of mesometrial tumor nodules are shown. Serial sections were stained with H&E, or with the indicated antibodies for immunohistochemistry. Ovaries are indicated (*), as are the oviduct (yellow arrow), the uterus (green arrow), and the tumor nodule (white arrow). Scale bar = 2mm